

NACA RM L53J20a



# RESEARCH MEMORANDUM

AN INVESTIGATION OF THE TRANSONIC AREA RULE BY FLIGHT  
TESTS OF A SWEEPBACK WING ON A CYLINDRICAL BODY  
WITH AND WITHOUT BODY INDENTATION BETWEEN  
MACH NUMBERS 0.9 AND 1.8

By Sherwood Hoffman

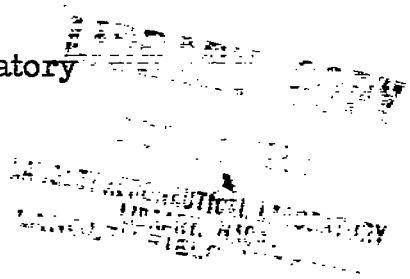
Langley Aeronautical Laboratory  
Langley Field, Va.

CLASSIFICATION CHANGED

UNCLASSIFIED

To: \_\_\_\_\_

By authority of NACA Res also effective  
YRN-121 Oct. 14, 1957  
Date \_\_\_\_\_



This material contains information affecting the National Defense of the United States within the meaning of the espionage laws, Title 18, U.S.C., Secs. 793 and 794, the transmission or revelation of which in any manner to an unauthorized person is prohibited by law.

## NATIONAL ADVISORY COMMITTEE FOR AERONAUTICS

WASHINGTON  
December 8, 1953

[REDACTED]  
NATIONAL ADVISORY COMMITTEE FOR AERONAUTICS

RESEARCH MEMORANDUM

AN INVESTIGATION OF THE TRANSONIC AREA RULE BY FLIGHT  
TESTS OF A SWEEPBACK WING ON A CYLINDRICAL BODY  
WITH AND WITHOUT BODY INDENTATION BETWEEN  
MACH NUMBERS 0.9 AND 1.8

By Sherwood Hoffman

SUMMARY

An investigation of the transonic area rule has been conducted by flight tests of a sweptback-wing—cylindrical-body configuration with and without a fuselage indentation and of their corresponding equivalent bodies of revolution through a range of Mach number from 0.9 to 1.8. The flight tests are compared with previous tests of similar models in the Langley 8-foot transonic tunnel. The wing had an angle of sweep of  $45^\circ$  along the quarter-chord line, an aspect ratio of 4.0, a taper ratio of 0.6, and an NACA 65A006 airfoil section in the free-stream direction. The cylindrical body had a fineness ratio of about 12.

Good agreement was obtained between the flight and tunnel data through most of the transonic speed range. Indenting the fuselage of the wing-body combination, in order to reduce the axial distribution of cross-sectional area to that of the original fuselage alone, resulted in a large reduction in drag rise between Mach numbers 0.95 and 1.18. This indentation produced a large increase in drag above Mach number 1.18. Near Mach number 1.0, the drag rise of the fuselage alone was approximately equal to the drag rise of the wing-body configuration with the indentation, whereas the drag rise from the body of revolution with the bump was only 60 percent of that for the basic wing-body configuration.

INTRODUCTION

The design of high-speed aircraft for minimum drag rise near the speed of sound has been greatly enhanced by the concepts of the transonic area rule of reference 1. Investigations of the area rule by wind-tunnel tests (refs. 1 to 4) of several wing-body configurations and of their

[REDACTED]

equivalent bodies of revolution have shown that the drag rise near Mach number 1.0 varied approximately with the rate of development of cross-sectional areas. Because there is little information available at present regarding the limitations of this rule, additional tests are being conducted to study the concepts of the area rule in more detail.

Tests of several configurations, including delta and straight-wing-fuselage combinations (ref. 1), have shown that the gains obtained by designing for an optimum area distribution at Mach number 1.0 were not limited to Mach number 1.0 but extended into supersonic speeds. The flight models of this investigation are similar to the sweptback-wing-cylindrical-fuselage models (ref. 1) tested in the Langley 8-foot transonic tunnel at Mach number 1.1. The present tests are compared with the transonic-tunnel data and extended the test Mach number range from 0.9 to 1.8. The corresponding Reynolds numbers vary from  $4 \times 10^6$  to  $11 \times 10^6$ , based on wing mean aerodynamic chord. One object of this extension is to determine if the favorable drag obtained at transonic speeds from this swept-wing configuration is also obtained at supersonic speeds.

#### SYMBOLS

A	cross-sectional area, sq ft
a	tangential acceleration, ft/sec <sup>2</sup>
$C_D$	drag coefficient, $C_{D_T} - C_{D_B} - C_{D_{fins}}$ , based on $S_W$
$C_{D_T}$	total drag coefficient, based on $S_W$
$C_{D_B}$	base drag coefficient, based on $S_W$
$C_{P_B}$	base pressure coefficient
$\bar{c}$	mean aerodynamic chord of wings, ft
g	acceleration due to gravity, 32.2 ft/sec <sup>2</sup>
L	length of configuration, ft
M	free-stream Mach number
p	free-stream static pressure, lb/sq ft

$P_B$	base pressure, lb/sq ft
$q$	free-stream dynamic pressure, lb/sq ft
$R$	Reynolds number, based on $\bar{c}$
$S_W$	total plan-form area of wing, sq ft
$S_B$	base area of fuselage, sq ft
$W$	weight of model during deceleration, lb
$X$	station measured from fuselage nose, ft
$\theta$	angle between flight path and horizontal, deg

#### MODELS

Details and dimensions of the four models flight tested are given in figure 1 and tables I to IV. These models without their stabilizing fins were similar to the series of sweptback-wing—cylindrical-body models tested in the Langley 8-foot transonic tunnel (ref. 1). The cross-sectional area distributions and photographs of the models are presented in figures 2 and 3, respectively.

The basic configuration, model A, consisted of a  $45^\circ$  sweptback wing mounted on an ogive-cylinder fuselage. The wing was located on the cylindrical afterbody of the fuselage (fig. 1) so that design modifications, based on the concepts of the area rule, can be made on the fuselage without changing the shape of the ogive nose. The wing had an angle of sweep of  $45^\circ$  along the quarter-chord line, an aspect ratio of 4.0 (based on total wing plan-form area), a taper ratio of 0.6, and an NACA 65A006 airfoil section in the free-stream direction. The ratio of total wing plan-form area to fuselage frontal area was 13.0. Model B, which consisted of the sweptback wing on the fuselage with an axially symmetrical indentation, had the same distribution of cross-sectional area as the ogive-cylinder fuselage alone. Model C consisted of the ogive-cylinder body with a symmetrical bump and had the same distribution of cross-sectional area as the basic wing-body configuration. Model D was the ogive-cylinder body alone.

Each model was stabilized by four fins as is shown in figures 1 and 3. The fins were flat plates, 0.091 inch thick with 0.045-inch radius at the edges. The leading edges of the fins were swept back  $45^\circ$ .

An NACA two-channel telemeter for transmitting longitudinal accelerations and base pressures was installed in the nose of each model. The base pressures were obtained from eight manifolded orifices (0.04-inch diameter) equally spaced on a tubular ring located 0.87 inch from the base of each model, as is shown in figure 1.

#### TEST AND MEASUREMENTS

The rocket-propelled zero-lift models were tested at the Langley Pilotless Aircraft Research Station at Wallops Island, Va. Each model was propelled from a zero-length launcher (fig. 3(a)) to supersonic speeds by a two-stage rocket system. The first stage or booster stage for the configurations with wings (models A and B) consisted of a fin-stabilized 6-inch ABL Deacon rocket motor. The booster stage for the configurations without wings (models C and D) consisted of a 5-inch-diameter, lightweight, high-velocity, aircraft rocket motor with fins. For the second stage, a 3.25-inch MK 7 rocket motor was installed in the fuselage of each model. Velocity and trajectory data were obtained from the CW Doppler velocimeter and the NACA modified SCR 584 tracking radar unit, respectively. The two-channel telemeter installed in the nose of each fuselage transmitted a continuous record of longitudinal accelerations and base pressures from the models to a ground-receiving station. A survey of atmospheric conditions was made by radiosonde measurements from an ascending balloon that was released at the time of each launching.

The flight tests covered a continuous range of Mach number from 0.9 to 1.8. The corresponding range of Reynolds number varied from approximately  $4 \times 10^6$  to  $11 \times 10^6$ , based on wing mean aerodynamic chord, as is shown in figure 4.

The values of total drag coefficient and base drag coefficient, based on total-wing plan-form area, were obtained during decelerating flight by use of the expressions

$$C_{DT} = - \frac{W}{qS_W} (a + g \sin \theta)$$

and

$$C_{DB} = \frac{P_B - P}{q} \frac{S_B}{S_W}$$

where  $S_B/S_W = 0.0768$ .

The drag coefficients of the configurations were obtained by subtracting the base drag and fin drag coefficients from the total drag coefficients as follows:

$$C_D = C_{D_T} - C_{D_B} - C_{D_{fins}}$$

where  $C_{D_{fins}}$  is based on  $S_w$ . The drag of the fins plus interference (fig. 5(a)) on the cylindrical fuselage was obtained from unpublished flight data. Estimates indicate that the fin-plus-interference drag would be approximately the same on all the models tested herein.

In reducing the present data, the probable errors in total drag coefficient were determined from comparison of  $C_{D_T}$  as determined from accelerations measured by the accelerometers in the models and accelerations obtained from differentiating the velocity-time curves of the CW Doppler velocimeter. The true airspeeds of the models were obtained by correcting the Doppler velocity measurements for winds aloft, thus minimizing the errors in  $M$  and  $q$ . The measurements of base pressure and atmospheric pressure were accurate to about 0.07 lb/sq in. From these considerations, the probable errors in the measured values (coefficients are based on total plan-form area of the wing) are believed to be as follows:

$C_{D_T}$ ( $1.05 \leq M \leq 1.8$ )	±0.0005
$C_{D_T}$ ( $0.9 \leq M \leq 1.05$ )	±0.0010
$C_{D_B}$ ( $1.05 \leq M \leq 1.8$ )	±0.0008
$C_{D_B}$ ( $0.9 \leq M \leq 1.05$ )	±0.002
$C_{P_B}$ ( $1.05 \leq M \leq 1.8$ )	±0.013
$C_{P_B}$ ( $0.9 \leq M \leq 1.05$ )	±0.030
$M$ ( $0.9 \leq M \leq 1.8$ )	±0.005

## RESULTS AND DISCUSSION

Faired curves showing the variations of the total drag coefficients and base pressure coefficients obtained from the flight tests are shown in figure 5. The total drag coefficients, less the base drag and fin drag coefficients, are presented in figure 6 as the variation of  $C_D$  with  $M$ . In figure 7, the drag coefficients are compared with  $C_D$

obtained from transonic wind-tunnel tests (ref. 1) of configurations that were similar to the flight models. The wind-tunnel data were obtained at a Reynolds number of about  $2 \times 10^6$ , which is approximately half of the Reynolds numbers obtained from flight over the comparable Mach number range. A comparison of the results in figure 7 shows that reasonably good agreement was obtained in the variations of  $C_D$  between the flight and tunnel tests through most of the transonic speed range. The slight differences in the magnitude of  $C_D$  shown in figure 7 probably resulted from the different methods employed in the two test facilities. The drag-rise coefficients of the flight models are presented in figure 8 for comparison with the cross-sectional area distributions of the configurations in figure 2.

The models tested in this investigation and reference 1 were designed to investigate the concepts of the transonic area rule. Indenting the fuselage of the wing-body configuration, in order to reduce cross-sectional area distribution to that of the cylindrical body alone, resulted in a large reduction in  $C_D$  between Mach numbers 0.95 and 1.18. At Mach number 1.0, the indentation produced a 28-percent reduction in drag (fig. 6) and a 74-percent reduction in drag rise (fig. 8). However, above Mach number 1.18, this indentation resulted in a large and undesirable increase in drag, which indicates a definite limitation to the application of the transonic area rule for this configuration. Reference 4 shows a favorable effect from an indentation on drag of a delta-wing-body combination at moderate supersonic speeds. Preliminary studies and reference 5 indicate that an undesirable increase in the supersonic drag resulting from an indentation may be reduced by designing the indentation in such a way as to cancel effectively the wing area along Mach lines at low supersonic speeds and still maintain a substantial reduction in the transonic drag.

Figure 8 shows that the wing and indented cylindrical body (model B) and the cylindrical body (model D), which have the same distribution of cross-sectional area, have approximately the same drag rise near Mach number 1.0. The basic wing-body configuration (model A) and the cylindrical body and bump (model C) also have the same distribution of cross-sectional area, but model C had only 60 percent of the drag rise of model A. This same result was obtained from the comparable transonic tunnel tests of reference 1 and also from flight tests of an equivalent area model of an airplane with swept wings in reference 6. Tests of other wing-body configurations having straight and delta wings in references 1 and 6 show that very good agreement between the drag rise of the aircraft configurations and their equivalent bodies of revolution may be obtained especially when the wing is thin and has a low taper ratio and aspect ratio. On the basis of the foregoing comparisons, it is evident that the concepts of the transonic area rule may be employed to a limited extent for estimating the drag rise and the qualitative effects of design modifications on the zero-lift drag of swept-wing aircraft at transonic speeds.

## CONCLUSIONS

The results of an investigation of the transonic area rule by flight tests at zero lift of a sweptback-wing—cylindrical-body configuration with and without a fuselage indentation and of their equivalent bodies of revolution for a range of Mach number from 0.9 to 1.8 indicate the following conclusions:

1. Good agreement was obtained between the flight tests and transonic tunnel tests of similar models through most of the transonic speed range.

2. Indenting the fuselage of the wing-body combination, in order to reduce the axial distribution of cross-sectional area to that of the original fuselage alone, resulted in a large reduction in drag rise between Mach numbers 0.95 and 1.18. This indentation produced a large increase in drag above Mach number 1.18.

3. Near Mach number 1.0, the drag rise of the fuselage alone was approximately equal to the drag rise of the wing-body configuration with the indentation, whereas the drag rise from the body of revolution with the bump corresponding to the sweptback wing was only 60 percent of that for the basic wing-body configuration.

Langley Aeronautical Laboratory,  
National Advisory Committee for Aeronautics,  
Langley Field, Va., October 6, 1953.

## REFERENCES

1. Whitcomb, Richard T.: A Study of the Zero-Lift Drag-Rise Characteristics of Wing-Body Combinations Near the Speed of Sound. NACA RM L52H08, 1952.
2. Robinson, Harold L.: A Transonic Wind-Tunnel Investigation of the Effects of Body Indentation, As Specified by the Transonic Drag-Rise Rule, on the Aerodynamic Characteristics and Flow Phenomena of a 45° Sweptback-Wing-Body Combination. NACA RM L52L12, 1953.
3. Carmel, Melvin M.: Transonic Wind-Tunnel Investigation of the Effects of Aspect Ratio, Spanwise Variations in Section Thickness Ratio, and a Body Indentation on the Aerodynamic Characteristics of a 45° Sweptback Wing-Body Combination. NACA RM L52L26b, 1953.
4. Whitcomb, Richard T.: Recent Results Pertaining to the Application of the "Area Rule." NACA RM L53I15a, 1953.
5. Whitcomb, Richard T., and Fischetti, Thomas L.: Development of a Supersonic Area Rule and an Application to the Design of a Wing-Body Combination Having High Lift-to-Drag Ratios. NACA RM L53H31a, 1953.
6. Hall, James Rudyard: Comparison of Free-Flight Measurements of the Zero-Lift Drag Rise of Six Airplane Configurations and Their Equivalent Bodies of Revolution at Transonic Speeds. NACA RM L53J21a, 1953.

TABLE I.- COORDINATES OF NACA 65A006 AIRFOIL

Station, percent chord	Ordinate, percent chord
0	0
.5	.464
.75	.563
1.25	.718
2.5	.981
5.0	1.313
7.5	1.591
10.0	1.824
15.0	2.194
20.0	2.474
25.0	2.687
30.0	2.842
35.0	2.945
40.0	2.996
45.0	2.992
50.0	2.925
55.0	2.793
60.0	2.602
65.0	2.364
70.0	2.087
75.0	1.775
80.0	1.437
85.0	1.083
90.0	.727
95.0	.370
100.0	.013

L.E. radius: 0.229 percent c  
T.E. radius: 0.014 percent c

TABLE II.- COORDINATES OF CYLINDRICAL FUSELAGE

[Stations measured from fuselage nose]

Station, in.	Ordinate, in.
0	0
.4	.185
.6	.238
1.0	.342
2.0	.578
4.0	.964
6.0	1.290
8.0	1.577
12.0	2.074
16.0	2.472
20.0	2.772
24.0	2.993
28.0	3.146
32.0	3.250
36.0	3.314
40.0	3.334
79.7	3.334

TABLE III.- COORDINATES OF CYLINDRICAL FUSELAGE WITH INDENTATION

[Stations measured from fuselage nose]

Station, in.	Ordinate, in.
(a)	(a)
40.00	3.334
41.07	3.334
42.85	3.271
44.62	3.174
46.40	3.037
48.17	2.914
49.95	2.827
51.73	2.771
53.50	2.792
55.28	2.800
57.05	2.870
58.83	2.940
60.61	2.998
62.38	3.090
64.16	3.200
65.93	3.286
67.71	3.328
68.15	3.334
79.7	3.334

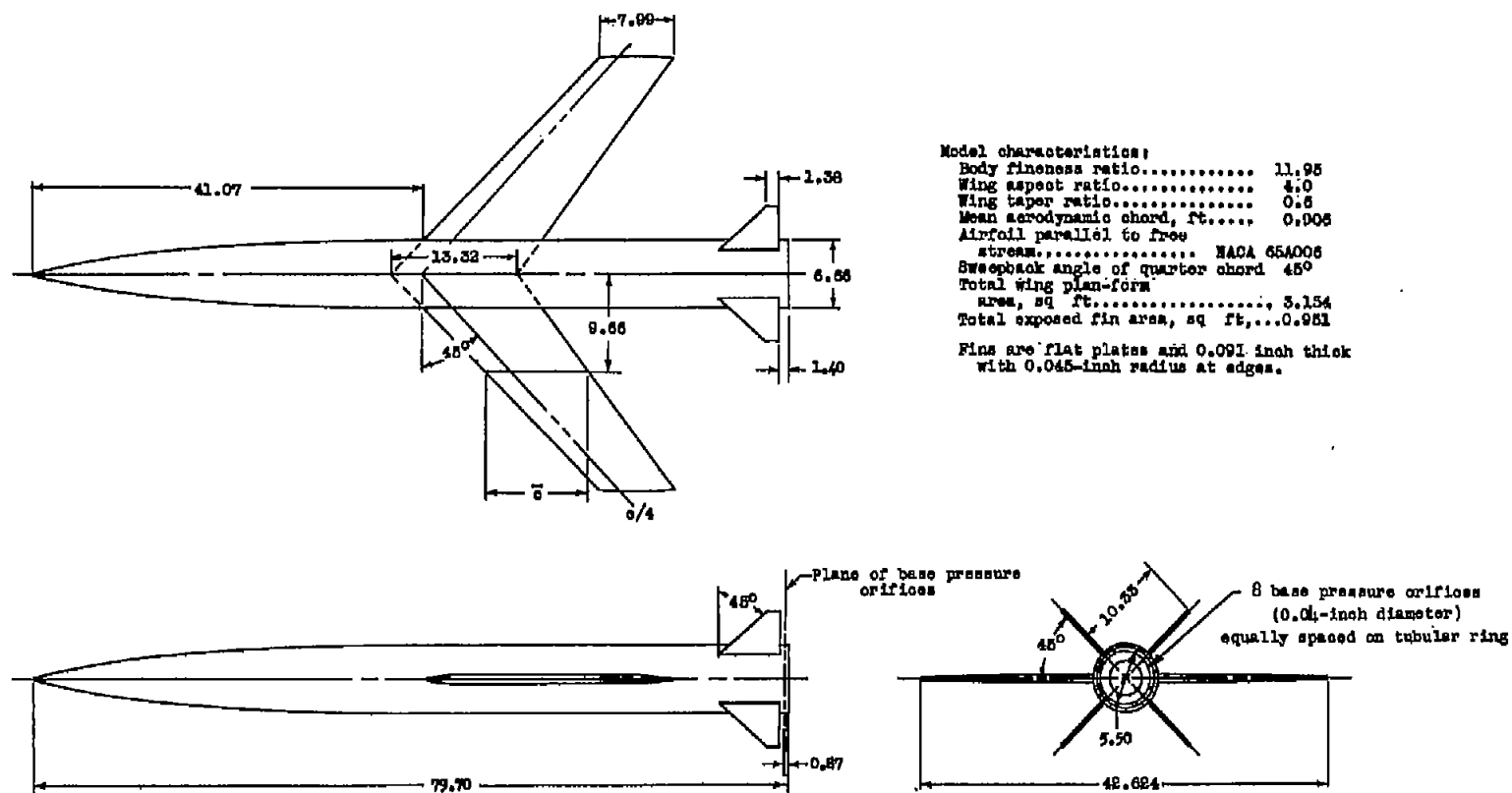
<sup>a</sup>Coordinates between stations 0 and 40 are identical to those of the cylindrical fuselage.

TABLE IV.- COORDINATES OF CYLINDRICAL FUSELAGE WITH BUMP

[Stations measured from fuselage nose]

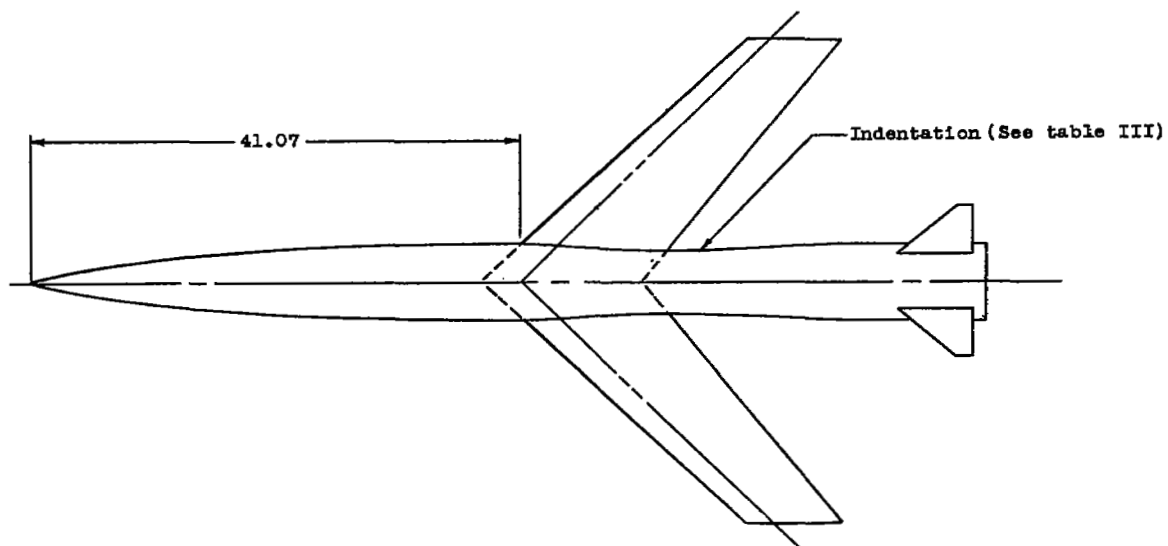
Station, in.	Ordinate, in.
(a)	(a)
40.00	3.334
41.07	3.334
42.85	3.387
44.62	3.476
46.40	3.595
48.17	3.694
49.95	3.760
51.73	3.806
53.50	3.792
55.28	3.760
57.05	3.720
58.83	3.678
60.61	3.632
62.38	3.554
64.16	3.456
65.93	3.373
67.71	3.347
68.15	3.334
79.7	3.334

<sup>a</sup>Coordinates between stations 0 and 40 are identical to those of the cylindrical fuselage.

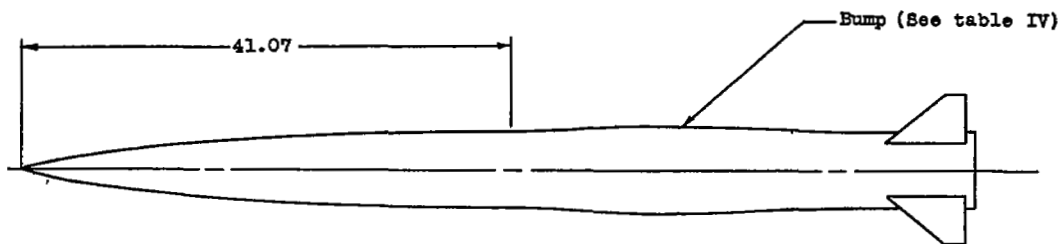


(a) Wing on cylindrical body (model A).

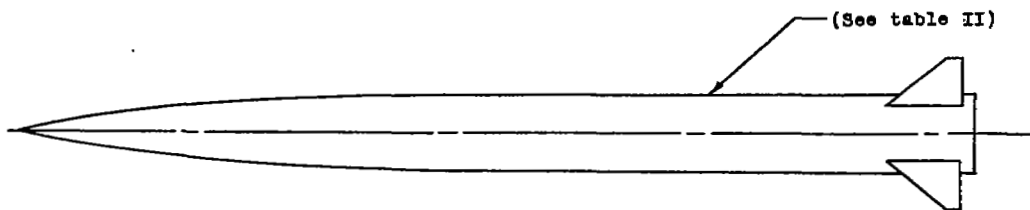
Figure 1.- Details and dimensions of test models. All dimensions are in inches.



(b) Wing on indented cylindrical body (model B).



(c) Bump on cylindrical body (model C).



(d) Cylindrical body (model D).

Figure 1.- Concluded.

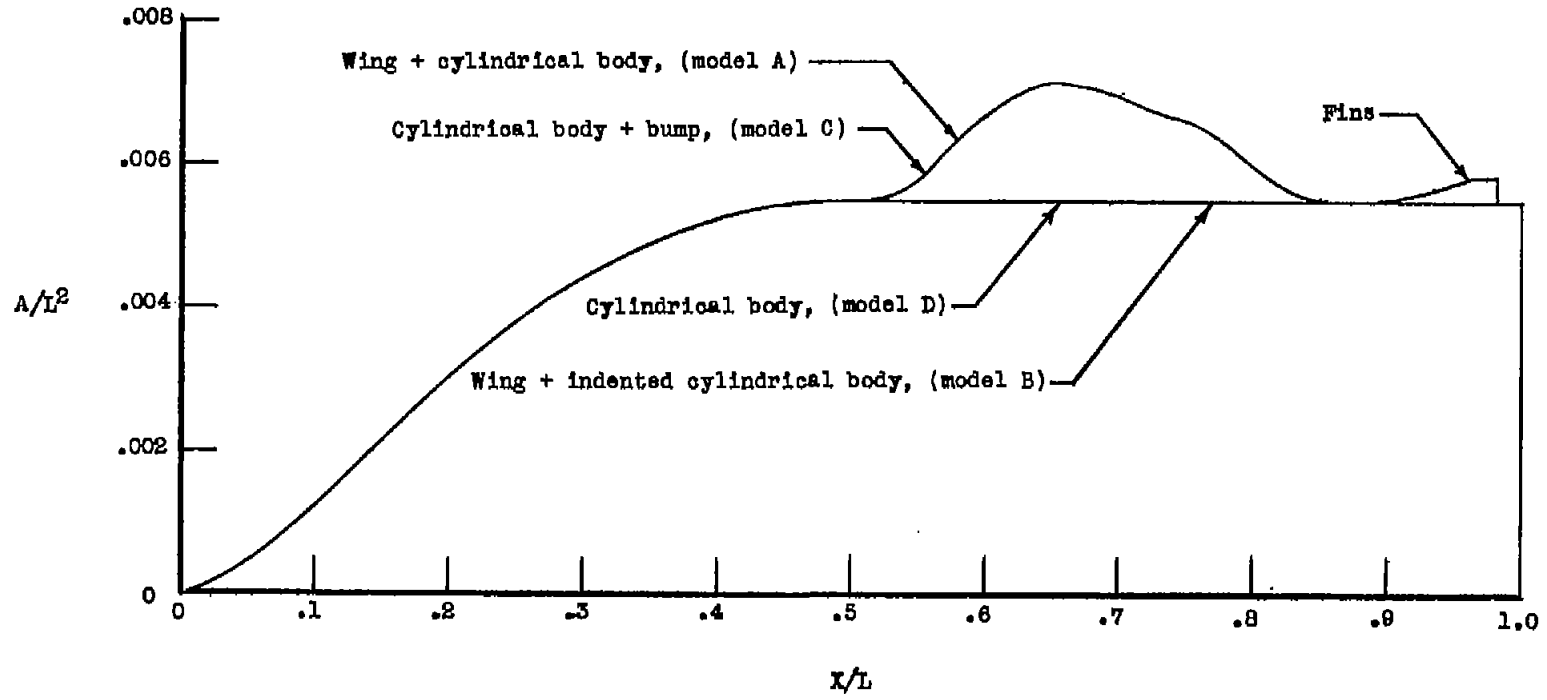
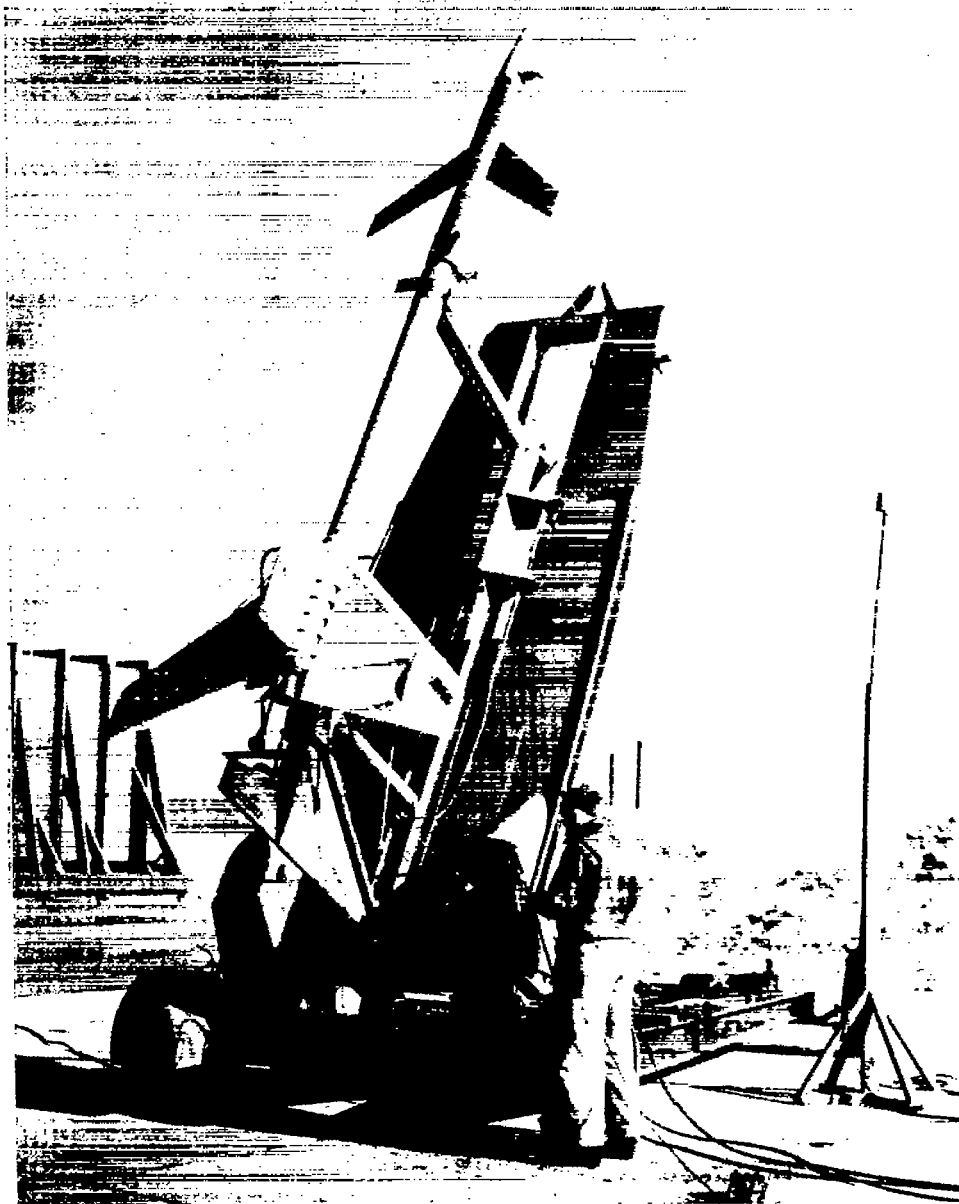


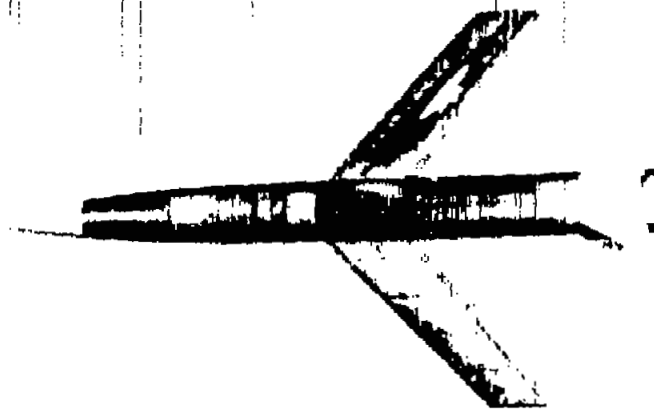
Figure 2.- Axial distribution of cross-sectional areas of models tested.



(a) Arrangement of model and booster on launcher.

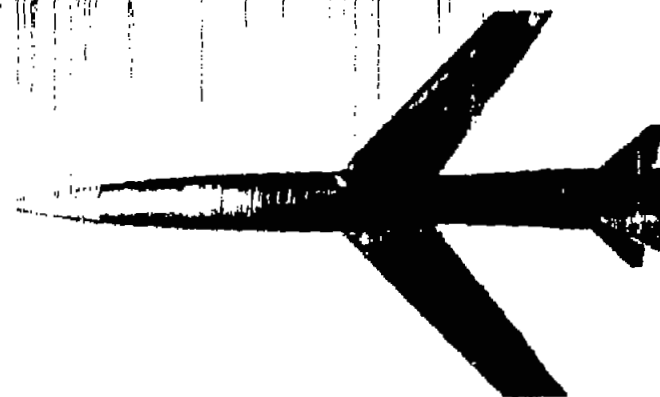
L-79175

Figure 3.- Photographs showing test models.



L-79419.1

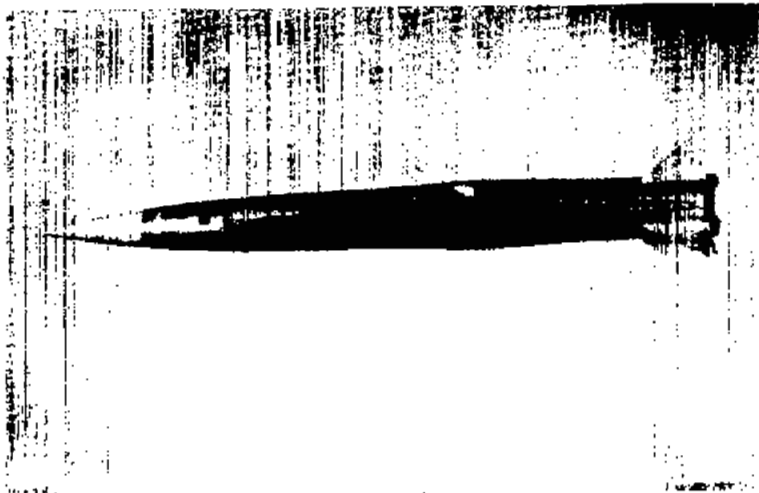
(b) Wing with cylindrical body  
(model A).



L-78972.1

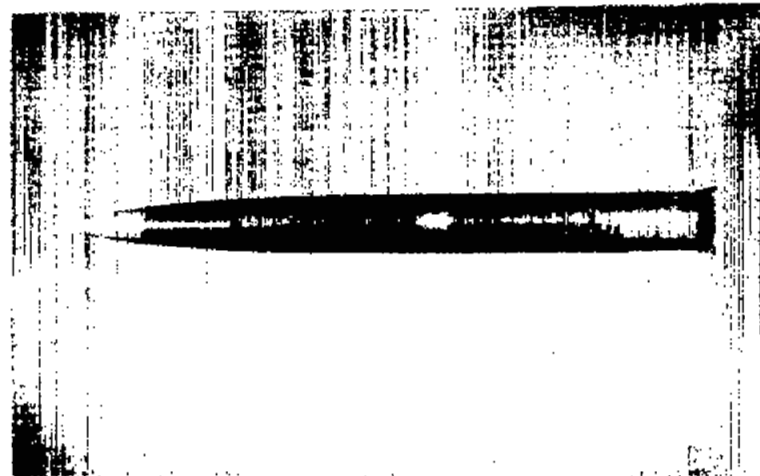
(c) Wing with indented cylindrical  
body (model B).

Figure 3.- Continued.



L-79418.1

(d) Cylindrical body with bump  
(model C).



L-79569.1

(e) Cylindrical body (model D).

Figure 3.- Concluded.

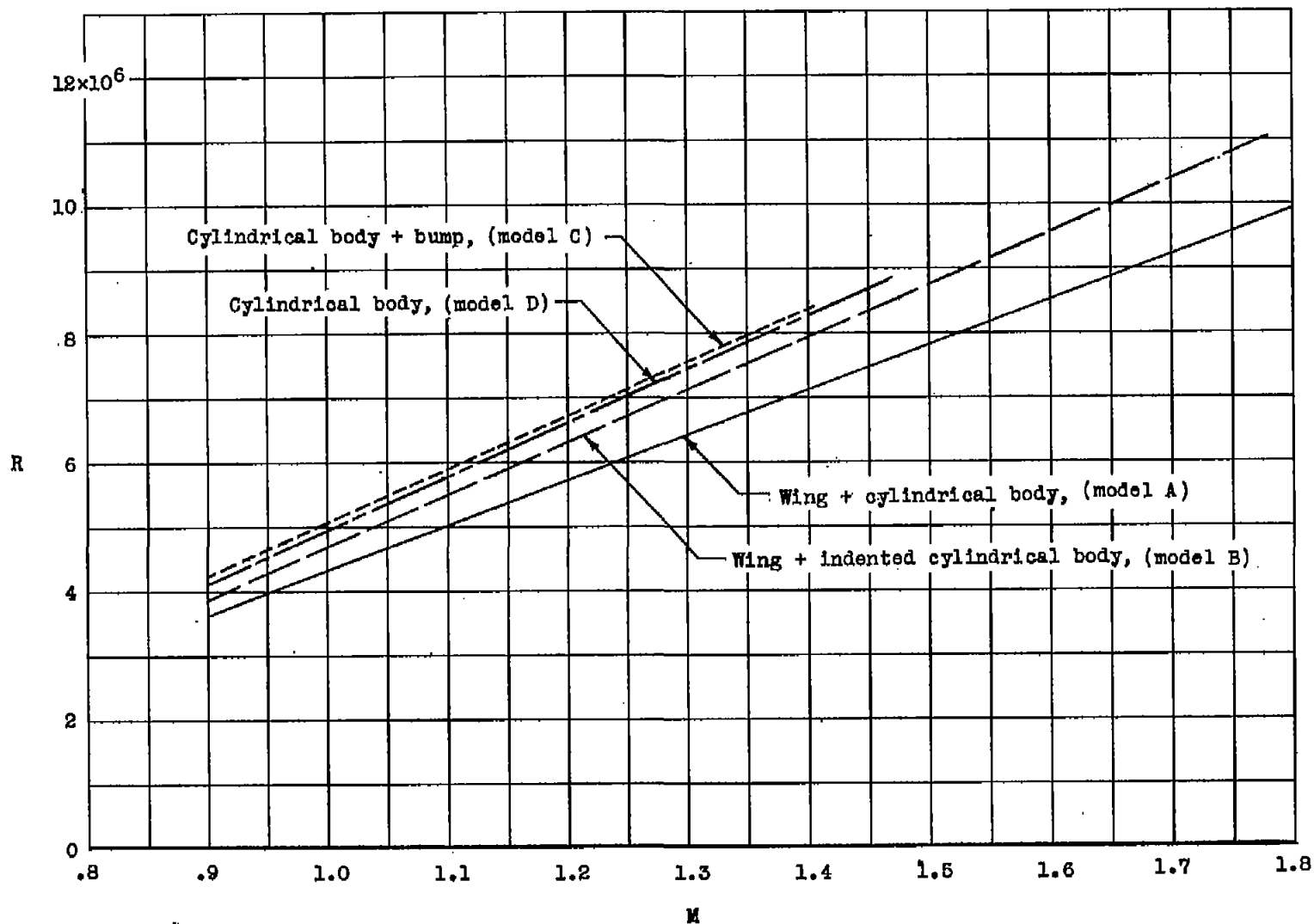
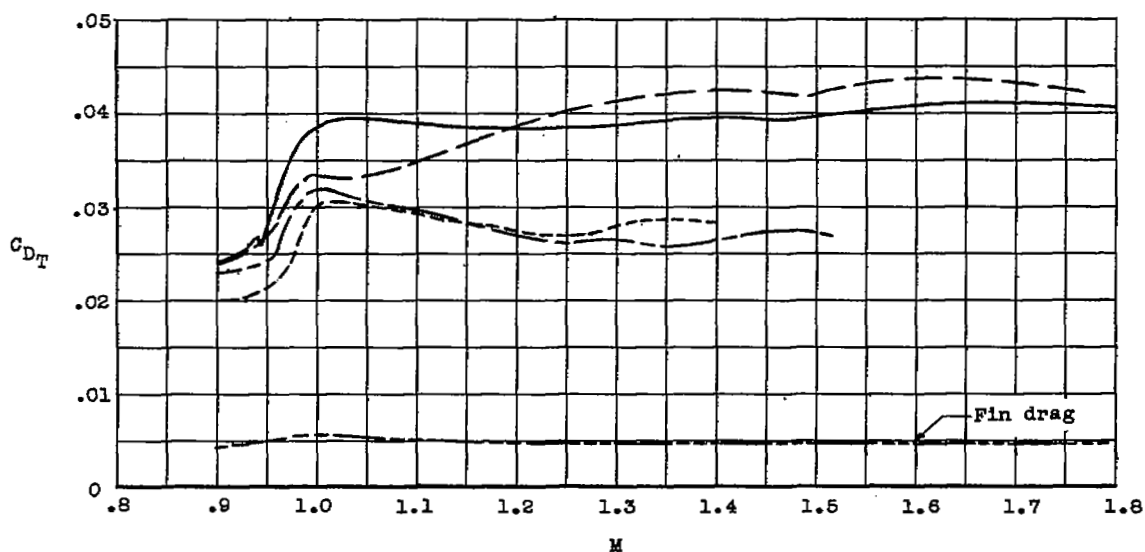
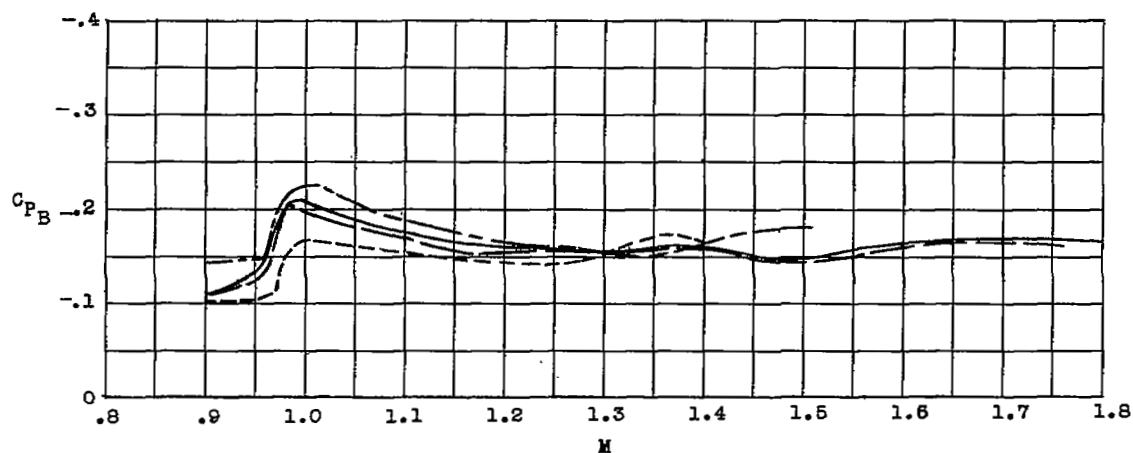


Figure 4.- Variation of Reynolds number with Mach number for models tested. Reynolds number is based on wing mean aerodynamic chord.

- \_\_\_\_\_ Wing + cylindrical body, (model A)  
 - - - - - Wing + indented cylindrical body, (model B)  
 - - - - - Cylindrical body + bump, (model C)  
 - - - - - Cylindrical body, (model D)



(a) Variation of total drag coefficient with Mach number.



(b) Variation of base pressure coefficient with Mach number.

Figure 5.- Variation of total drag coefficient and base pressure coefficient with Mach number for models tested.

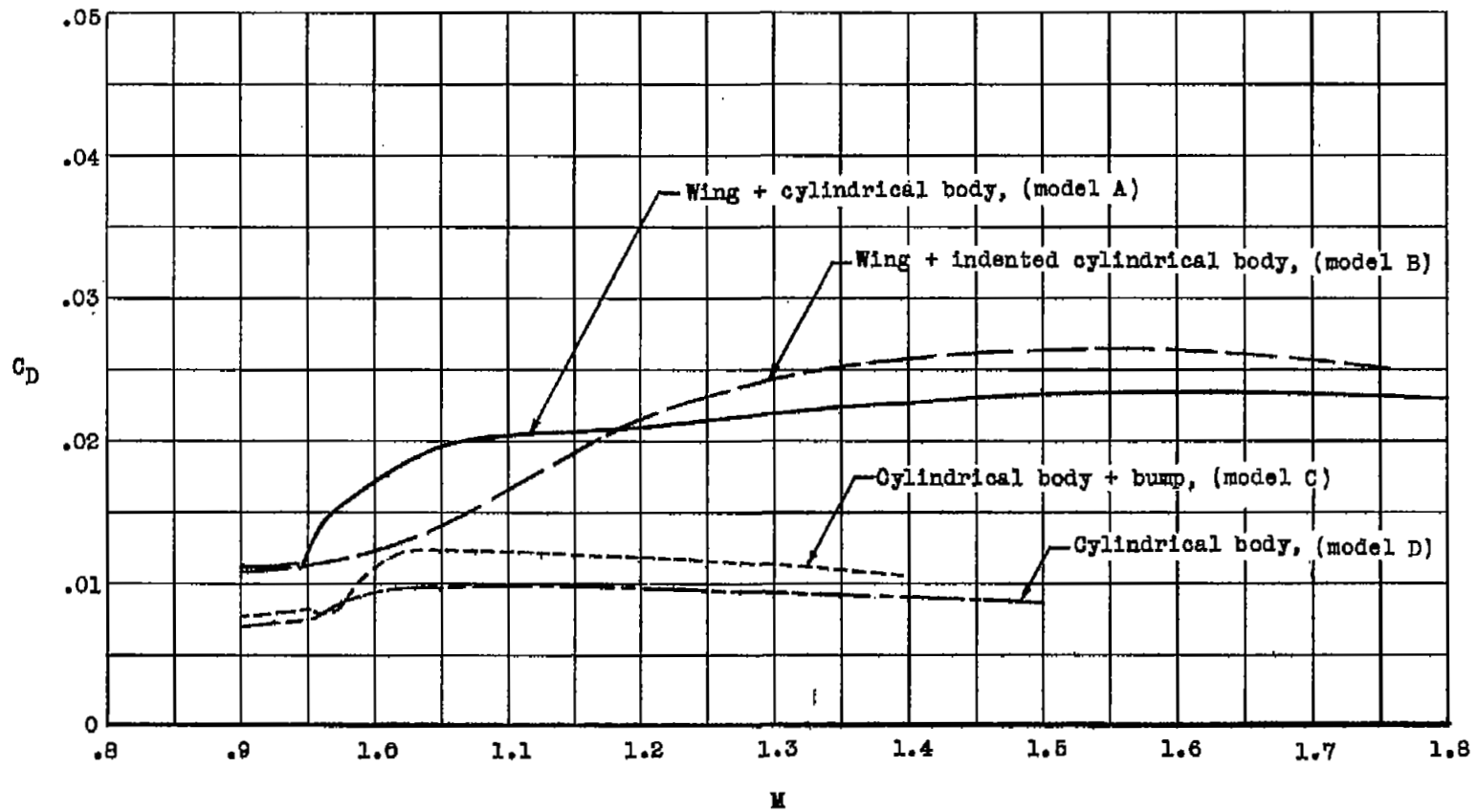
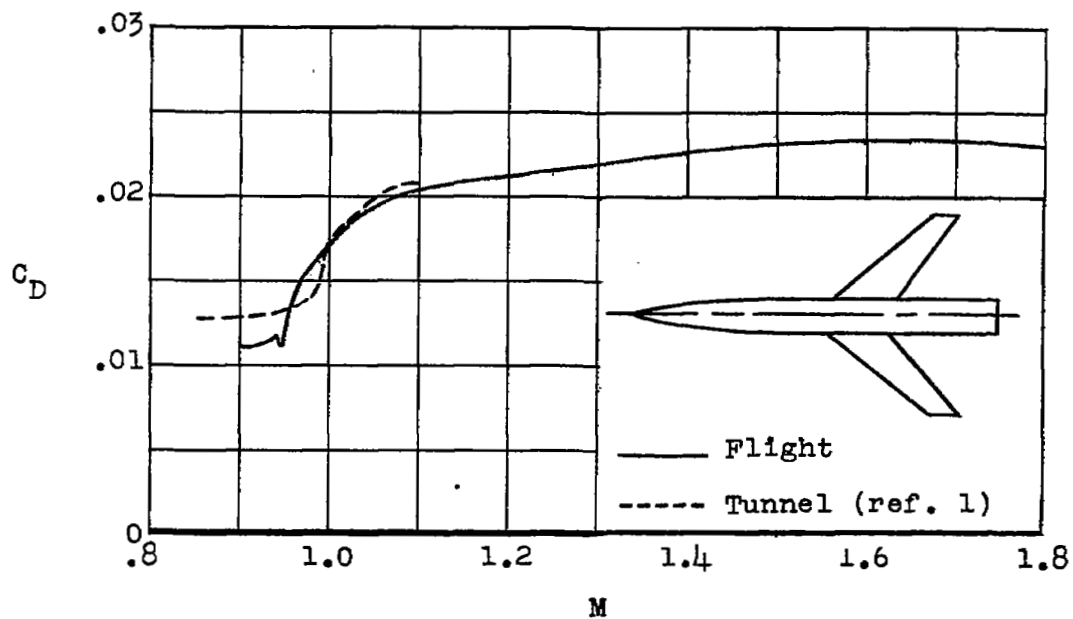
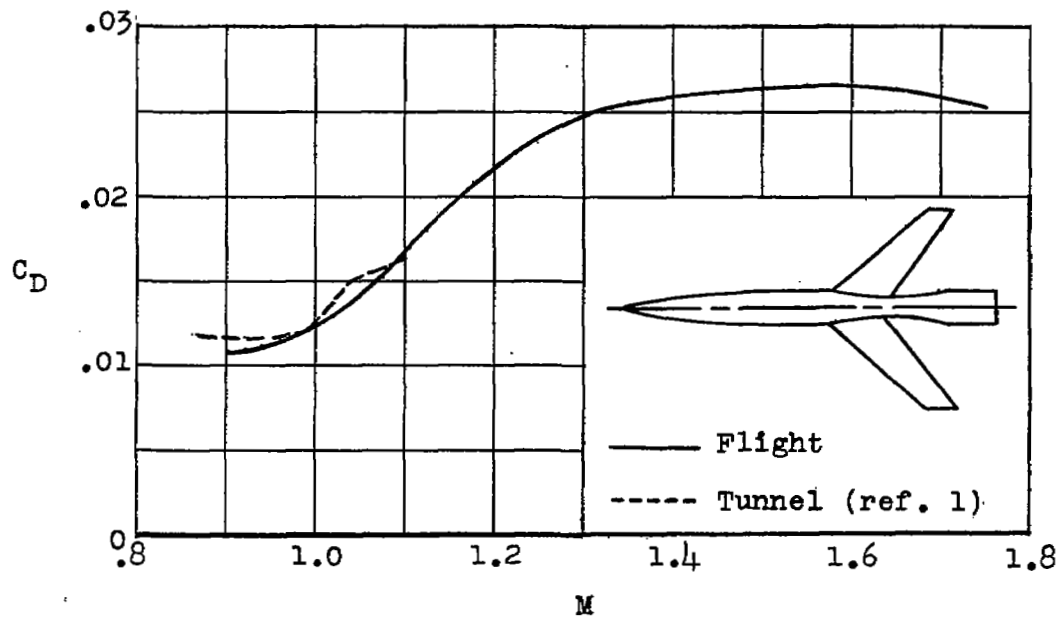


Figure 6.- Variation of drag coefficient with Mach number for the configurations tested. Fin drag coefficient is subtracted and base pressure is adjusted to free-stream static pressure.

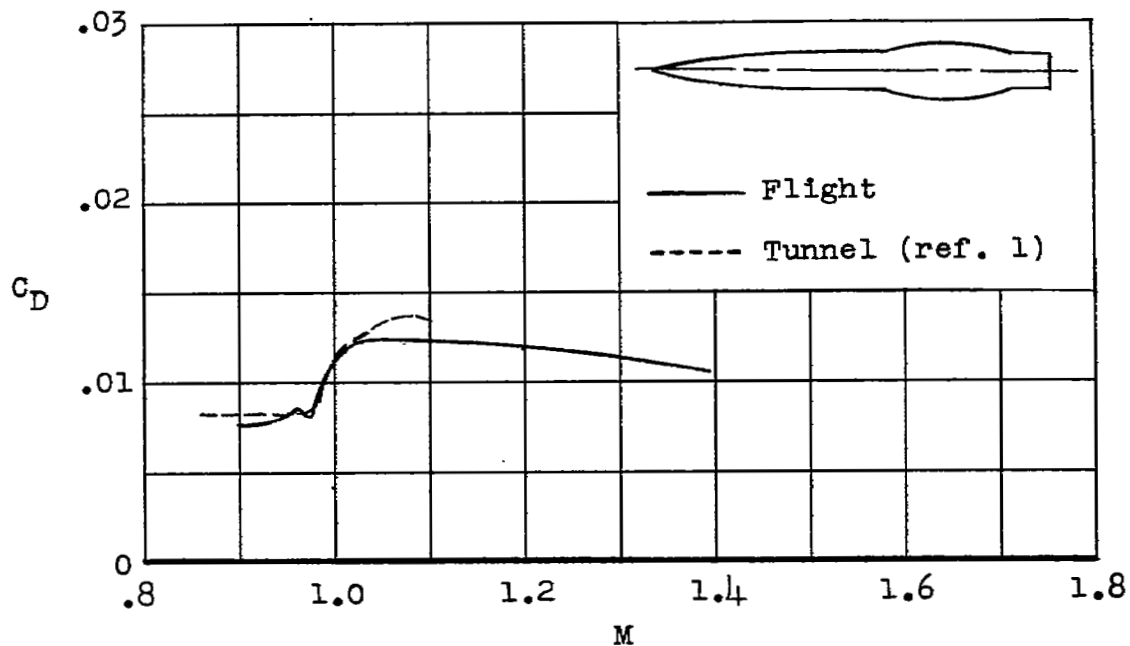


(a) Wing with cylindrical body.

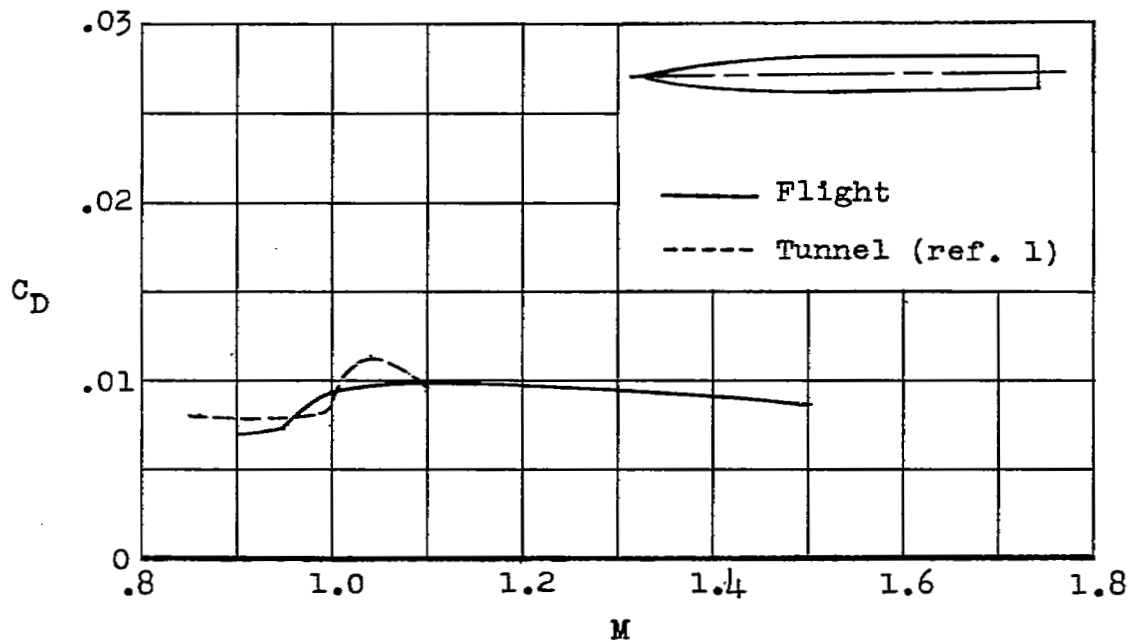


(b) Wing with indented cylindrical body.

Figure 7.- Comparison of variations of drag coefficient with Mach number for flight models and models tested in Langley 8-foot transonic tunnel (ref. 1).



(c) Cylindrical body with bump.



(d) Cylindrical body.

Figure 7.- Concluded.

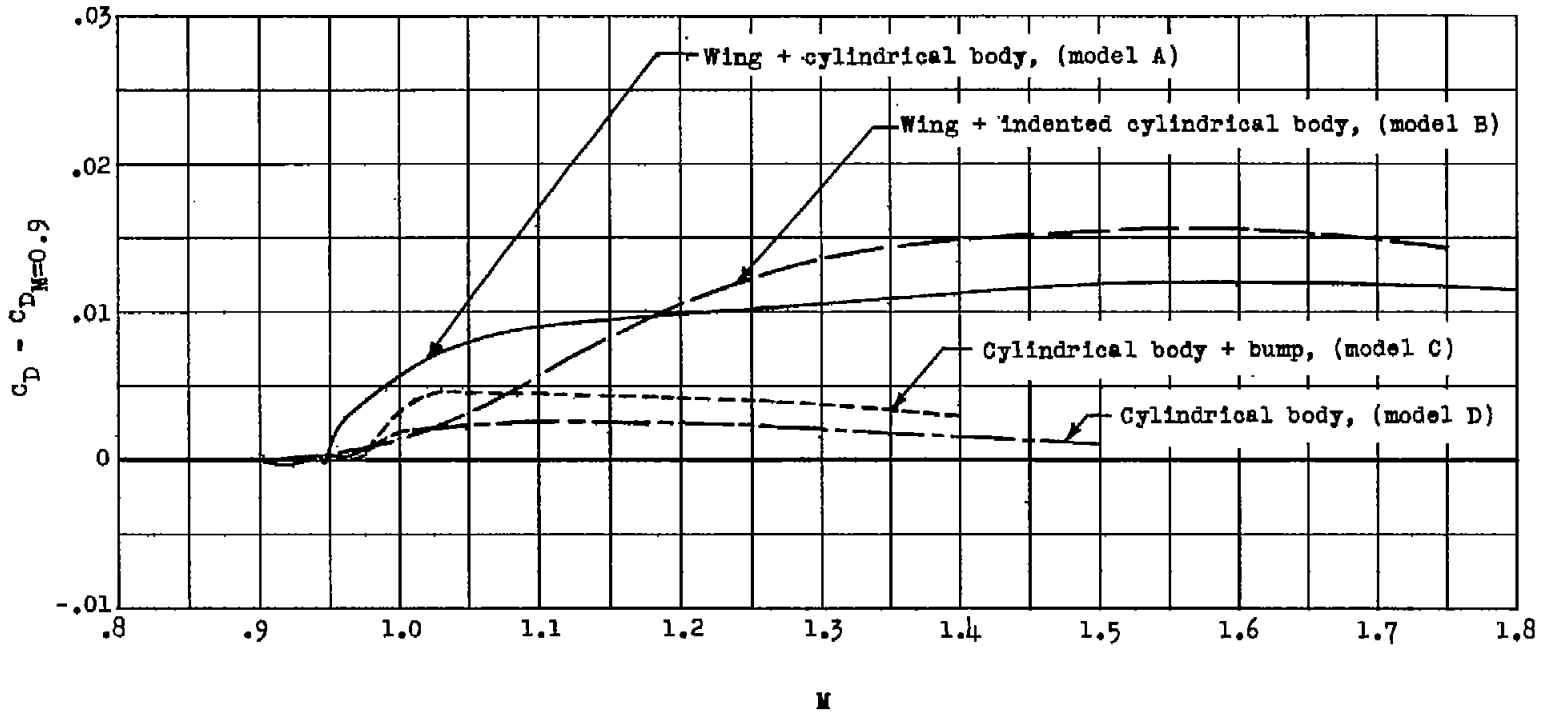
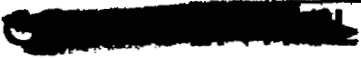


Figure 8.- Comparison of drag-rise coefficients of models tested.

SECURITY INFORMATION



LANGLEY RESEARCH CENTER



3 1176 01308 6906